Available online at www.sciencedirect.com
ScienceDirect
Journal of Nuclear Materials 356 (2006) 88–94
journal of nuclear materials
www.elsevier.com/locate/jnucmat

Recovery of tensile properties in helium implanted EUROFER97 by post-implantation annealing

P. Jung [a,*], J. Chen [b], H. Klein [a]

[a] Institut für Festkörperforschung, Forschungszentrum Jülich, D-52425 Jülich, Germany
[b] Department of Nuclear Energy and Safety, Paul Scherrer Institut, CH-5232 Villigen PSI, Switzerland

Abstract

Reduced activation martensitic stainless steel EUROFER97 was homogeneously implanted at 250 °C with 0.25 at.% helium, and was subsequently annealed in vacuum for 10 h at 550 °C and 750 °C, respectively. Tensile testing at room temperature and at 250 °C showed increase in strength and decrease of ductility by the implantation. Both changes recovered during annealing: While the strength was reduced by annealing to values between unimplanted and implanted condition, ductility was increased even beyond that of virgin material. This means, the implanted plus annealed material showed improved behaviour even when compared to the virgin material: higher strength and greater ductility. Including the results on fracture surface and microstructural investigations, a tentative model is presented.

1. Introduction

Low temperature embrittlement of structural materials under irradiation is one of the major concerns with respect to the use of ferritic/martensitic steels in fission and fusion reactors or high power spallation sources. Low temperatures are foreseen in liquid-mercury spallation targets (250 °C), but may also be encountered in some parts of high-temperature devices or during transients. Investigations on boron-doped martensitic steels showed enhanced increase in ductile-to-brittle transition temperature, which was ascribed to the production of helium by transmutation [1,2]. Strong embrittlement was also revealed by tensile tests on helium implanted materials [3,4]. The observation that irradiation hardening of ferritic/martensitic steels ceases at irradiation temperatures above 400 °C, lead to the proposition to use annealing treatment for extending the lifetime of structural components, cf. Ref. [5]. Previous Charpy V-notch tests on 9–12% Cr steels, irradiated in fast reactors at around 300 °C showed significant recovery of upper-shelf energy (USE) after annealing around 550 °C [6–8]. Other mechanical studies in literature on effects of annealing of irradiated metals are limited to copper and Cu-alloys [9–12], and therefore are not directly comparable to steels. Recent tests on steel specimens which were accidentally annealed during irradiation [13] and on various materials irradiated in spallation sources [14] showed significant recovery of tensile properties

* Corresponding author. Tel.: +49 2461 614036; fax: +49 2461 614413.
E-mail address: p.jung@fz-juelich.de (P. Jung).

0022-3115/$ - see front matter © 2006 Elsevier B.V. All rights reserved.
doi:10.1016/j.jnucmat.2006.05.005

after post-irradiation annealing. As high helium production rates are characteristic for irradiation mainly in spallation sources, it was the aim of the present work to study the effect of annealing after implantation to high helium concentrations on tensile properties of a martensitic steel, and to relate the mechanical behaviour to microstructural development.

2. Material

The reduced activation martensitic stainless steel EUROFER97 was obtained from the European fusion materials programme in the form of 9 mm plates, with the major constituents (wt%, bal. Fe) C: 0.11, N: 0.03, P: 0.005, V: 0.2, Cr: 9.0, Mn: 0.48, Ni: 0.021, Nb: 0.0017, Ta: 0.07, W: 1.1. Sheets of 0.4 mm thickness were cut by spark erosion and were cold-rolled to 100 μm in steps of 25% reduction with intermediate anneals at 750 °C for 1 h in vacuum. Dog-bone shaped specimens with gauge length of 12 mm, width of 2 mm, fillet radii of 1 mm and grip width of 8 mm were cut by spark erosion. Final heat treatment was 1/2 h at 980 °C with fast cooling to room temperature and normalising for 1 1/2 h at 750 °C and slowly cooling in the furnace.

3. Implantation

Four specimens were mounted vertically side by side, with only the lower grips fixed, and the upper ones free to avoid thermal stresses during implantation. One specimen had potential leads for temperature control by resistance measurement. The maximum energy of α-particles (^{4}He) obtained from the Jülich compact cyclotron CV28 behind a 25 mm Hasteloy window is about 23.9 MeV. giving ranges of about 110 μm in steels, according to TRIM–SRIM calculations [15]. Homogeneous implantation throughout this thickness was achieved by using a degrader wheel with 24 Al foils of appropriate thicknesses which varies the energy in front of the specimens from 0 to 23.9 MeV [3]. Thicknesses of the degrader foils were optimised for steel to obtain concentration inhomogeneities below 1%. Displacement production was calculated by TRIM with a displacement energy of 40 eV [16], and a binding energy E_b of 2 eV, giving at the front side of the specimen by about a factor of two higher defect production than at the back-side, with an average of 154 displacements per implanted ion, corresponding to 0.66 at.%He/dpa, i.e. a total dose of 0.38 dpa for a maximum helium concentration of 0.25 at.%, cf. Ref. [4]. Typical implantation rates were about 0.015 appm He/s, corresponding to 2.3×10^{-6} dpa/s. Implantation dose was derived from measurements of beam current on a shutter during beam-off periods. Beam stability during implantation was monitored by the signals of a four-quadrant aperture. Implantation dose was derived from the beam current after correction for secondary electrons by about 30% according to previous desorption experiments. Beam was wobbled across the specimens at about 250/s, spreading more than 50% of the beam to the four-quadrants to obtain fairly uniform distribution on the specimens. Uniformity of doses on all specimens was further improved by exchanging inner and outer specimens after half the total dose. The specimens were cooled from both sides by purified and thermostatised helium gas. The specimens were heated by the beam, with temperature adjustment by the flow rate of the helium. Temperature was measured by infrared pyrometry under 45° from the backside of the specimens, and average temperature was derived from resistance measurement on one specimen.

4. Testing

Post-implantation annealing was performed at 550 °C and 750 °C, respectively, for 10 h in vacuum better than 10^{-3} Pa with quick cooling to room temperature. The specimens were tensile tested in a device for miniature specimens, located in a vacuum furnace under 10^{-3} Pa. Testing was started after evacuation and heating within about 0.5 h at a strain rate of 8.5×10^{-5}/s. Fracture surfaces were analysed by scanning electron microscopy (SEM) using a Hitachi S-4100 at a voltage of typically 20 kV. Reduction of area $\Delta A/A_0$ of the foil specimens was approximated by the ratio of neck width (w_{neck}) to total thickness d by:

$$\Delta A/A_0 = 1 - w_{neck}/d. \quad (1)$$

Transmission electron microscopy was used for microstructural investigation, using a JEM 2010 of 200 keV electron energy. Specimens of 1 mm diameter were prepared after tensile testing and the disks were finally perforated by electrochemical thinning technique. Dislocation structure was studied by two-beam bright-field and weak-beam dark-field imaging, while helium bubbles were analysed by bright-field through-focus imaging.

5. Results

Fig. 1 shows stress–strain curves of pristine EUROFER97, after implantation at 250 °C to 0.25 at.% helium, and after annealing for 10 h at 550 °C and 750 °C, respectively. As already found previously [3,4] strength is increased and strain significantly reduced after helium implantation. Actually in the specimen tested at 250 °C, virtually no ductility is retained after implantation. On the

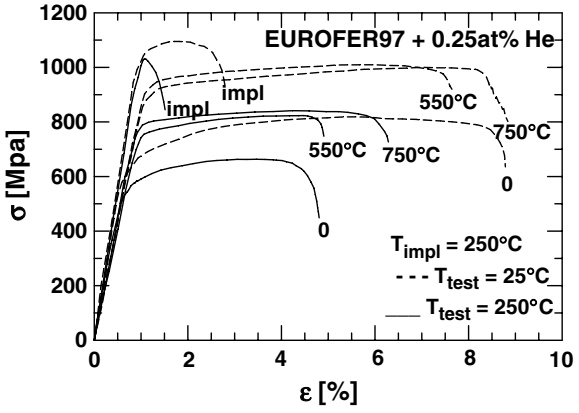

Fig. 1. Stress–strain curves of EUROFER97 before (0) and after implantation of 0.25 at.% helium at 250 °C, and after post-implantation annealing for 10 h at temperatures of 550 °C and 750 °C. The tensile tests were performed at a strain rate of 8.5×10^{-5}/s at temperatures of 25 °C and 250 °C, respectively.

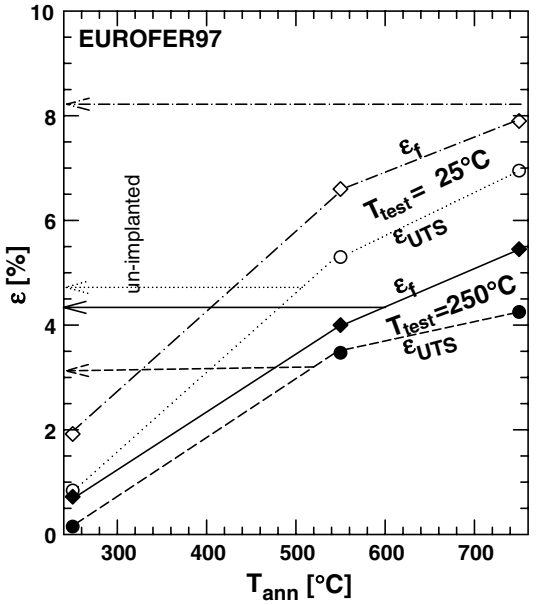

Fig. 3. Strains at ultimate tensile strengths and at fracture of EUROFER97 versus annealing temperature. Data at 250 °C indicate the as-implanted, arrows the unimplanted specimens. Lines are included to guide the eye.

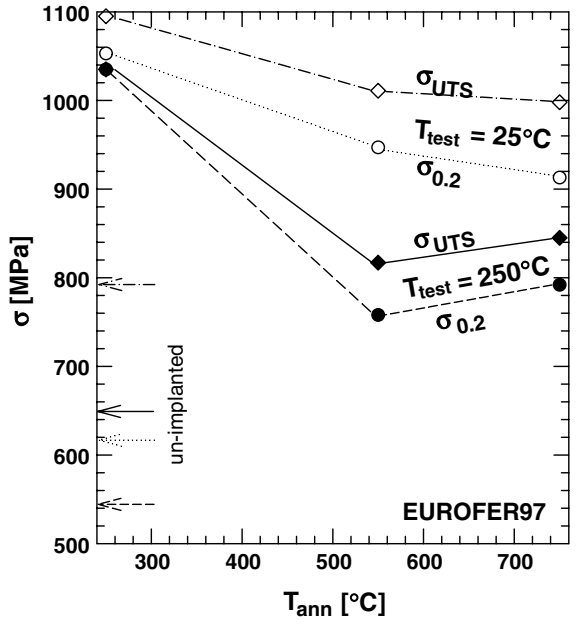

Fig. 2. Yield stresses (0.2% offset) and ultimate tensile strengths of EUROFER97 versus annealing temperature. Data at 250 °C indicate the as-implanted, arrows the unimplanted specimens. Lines are included to guide the eye.

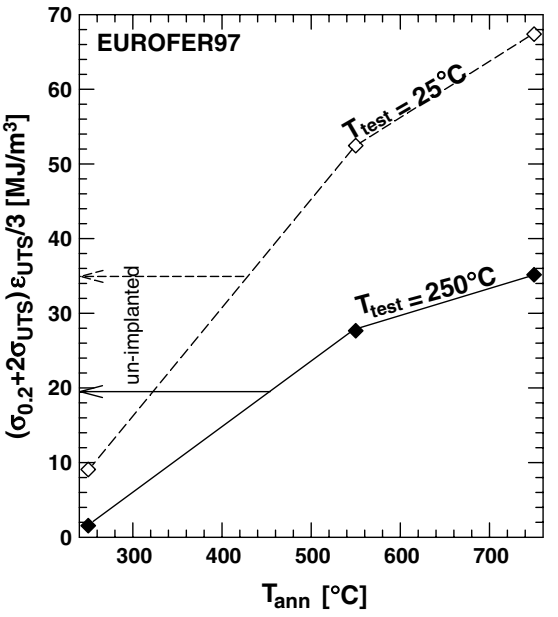

Fig. 4. Fracture energy density of EUROFER97 as defined by Eq. (2) versus annealing temperature. Data at 250 °C indicate the as-implanted, arrows the unimplanted specimens. Lines are included to guide the eye.

other hand, after annealing both at 550 °C and 750 °C, strength is reduced, but clearly stays above the un-implanted value. More important, the strain recovers to the original value or even beyond, and also some work hardening capability is regained. Yield stresses, ultimate tensile strengths, uniform elongations (taken at ultimate tensile stress), and total elongations as a function of annealing temperature are summarized in Figs. 2 and 3. Fracture energy density E_{UTS} can be defined by:

$$E_{UTS} = (\sigma_{0.2} + 2 \cdot \sigma_{UTS}) \cdot \varepsilon_{UTS}/3, \quad (2)$$

if a parabolic stress–strain relation is assumed in the plastic regime. Data in Fig. 4 show reduction of E_{UTS} by implantation, and again recovery beyond the original values already by annealing at 550 °C.

SEM images of fracture surfaces were taken from the centre of the necked region. Despite the severe reduction of elongation, the failure mode of EUROFER97 was still ductile after implantation, with some minor differences observed for testing at 25 °C (Fig. 5). Only implantation to 0.5 at.%He was previously found to cause a transition to completely brittle intergranular fracture [3]. After

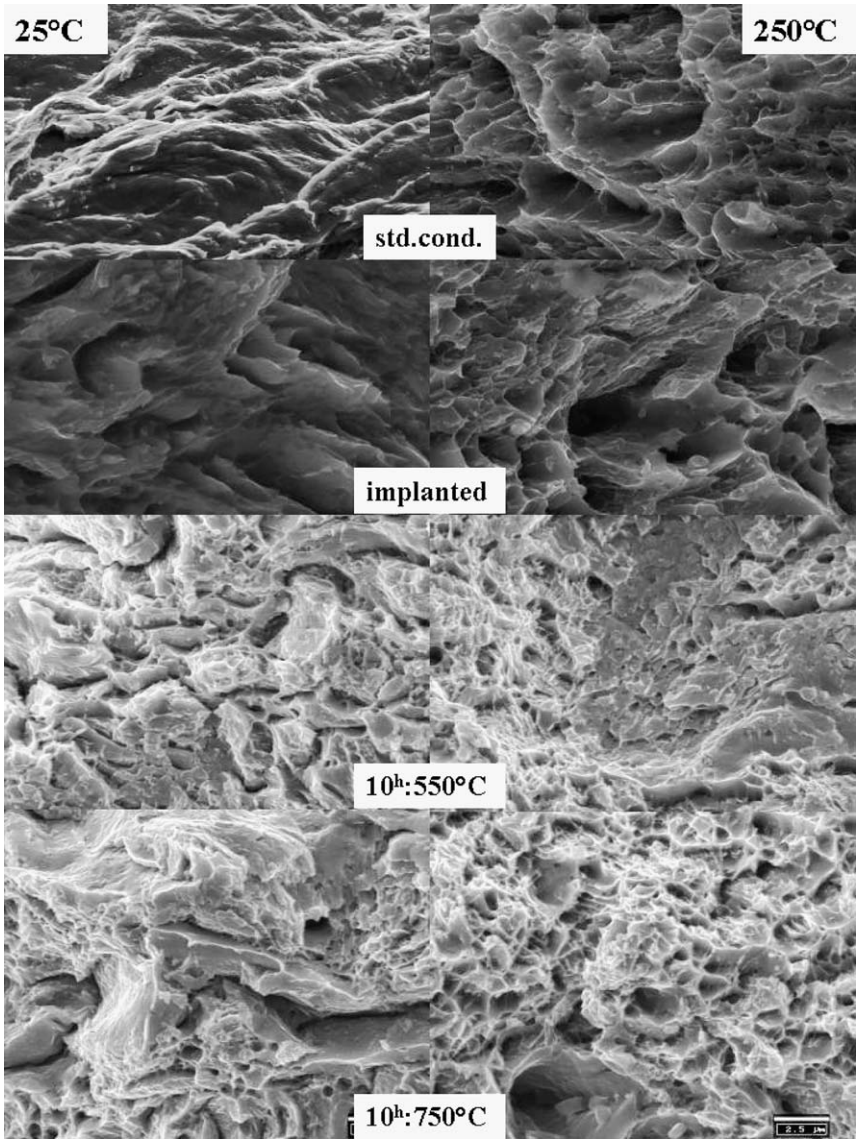

Fig. 5. Scanning electron micrographs of the fracture morphology of EUROFER97 in standard condition, after implantation of 0.25 at.% He at 250 °C and after annealing for 10 h at 550 °C and 750 °C, respectively.

annealing, the fracture surfaces show a pronounced dimple ductile-appearance. Data on reduction in area $\Delta A/A_0$ derived from the SEM micrographs according to Eq. (1), are shown in Fig. 6. $\Delta A/A_0$ is significantly reduced by implantation and shows minor changes only after annealing at 750 °C.

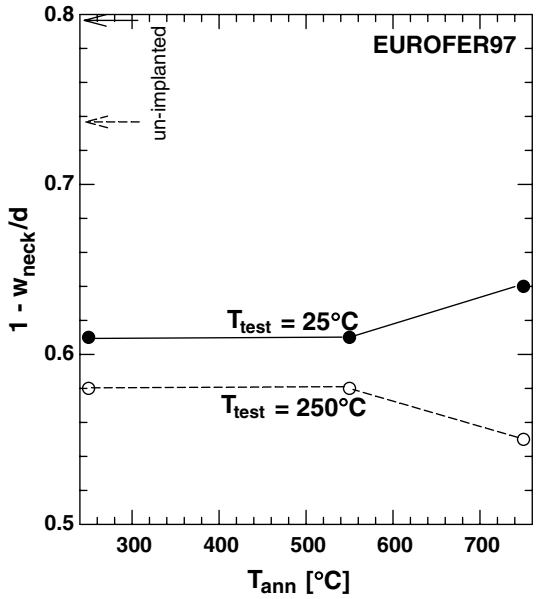

Fig. 6. Reduction in area of EUROFER97 versus annealing temperature, as derived from width at necking. Data at 250 °C indicate the as-implanted, arrows the unimplanted specimens. Lines are included to guide the eye.

After annealing at 550 °C as well as 750 °C, the microstructure observed consisted of high density of bubbles with average diameters of 1.5 (Fig. 7) and 1.7 nm, respectively. High density of 'black-dot' and small loop damage, which is a typical damage feature after implantation and irradiation at low temperatures [17,18], was not observed in the samples after post-implantation annealing. On the other hand, a high density of dislocations was observed. Since TEM specimen was punched out after tensile test, the dislocations produced by post-implantation annealing and by plastic deformation cannot be distinguished. A typical microstructure is shown in Fig. 8.

6. Discussion

The following topics will be addressed:

(1) Comparison of results to annealing after irradiation in a spallation source.
(2) Effect of helium concentration.
(3) Discussion of the results in view of hardening models.

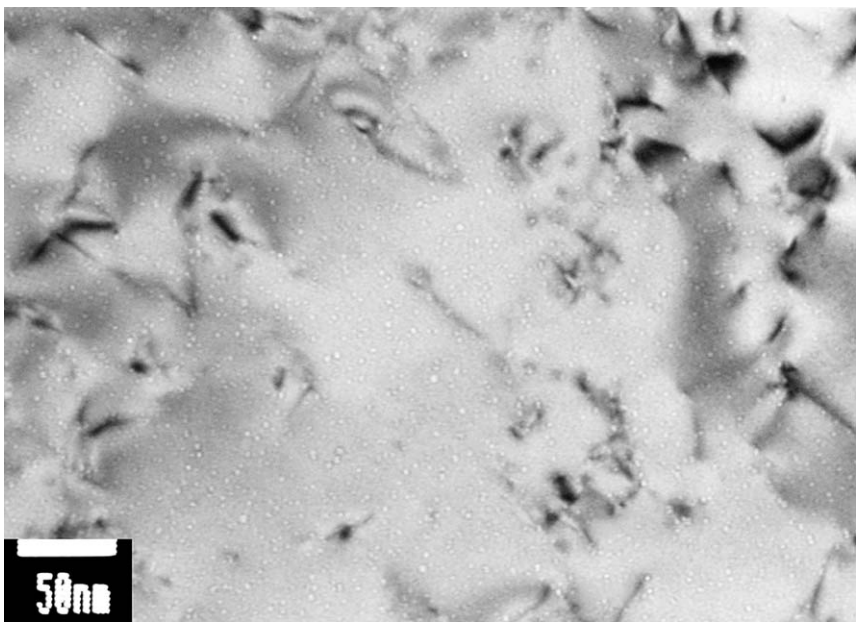

Fig. 7. Bubbles in EUROFER97, observed after implantation to 0.25 at.% He at 250 °C, annealing for 10 h at 550 °C, and testing at 250 °C. Average bubble diameter $D_b = 1.5$ nm.

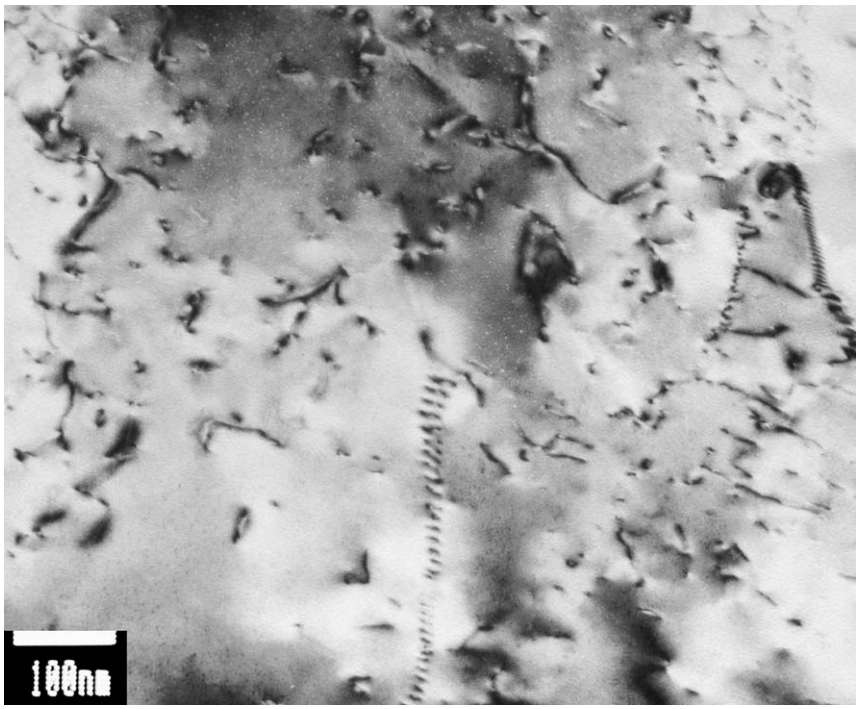

Fig. 8. Dislocation microstructure in EUROFER97, observed after implantation to 0.25 at.% He at 250 °C, annealing for 10 h at 750 °C, and testing at 250 °C.

(1) The effect of annealing on the tensile behaviour of 9% Cr EUROFER97 in the present investigations resembles the observations on 11% Cr DIN1.4926 irradiated in a spallation source (LANSCE, Los Alamos) with 800 MeV protons at $\leqslant$230 °C to a displacement dose of 5.8 dpa (2.8 Ah, i.e. 2.2×10^{25} p/m^2) and to a He concentration of 0.13 at.% [14]. In that study, different annealing temperatures up to 700 °C were applied, and reduction of strength and increase of ductility started after annealing just above the irradiation temperature, with recovery increasing with annealing temperature. The only major difference to the present results was, that after the 800 MeV proton irradiation $\Delta A/A_0$ was not significantly changed by irradiation and consequently also not by annealing. This difference may be ascribed to the higher specimen thickness (0.5 mm) and higher aspect ratio in Ref. [14], cf. Ref. [19]. It was shown in Ref. [14] that post-irradiation annealing improved strength and ductility also of austenitic AISI304L. While irradiation-induced degradation in tensile properties was less pronounced in the austenitic compared to the martensitic steel, 304 L showed changes of fracture mode by irradiation, which also recovered during annealing.

(2) The similarity in tensile results from He implantation and high-energy proton irradiation indicates a dominance of displacement defects in controlling mechanical properties, while specific effects of helium seem less pronounced. Also in Ref. [4] it was shown that at low doses, hardening is dominated by displacement defects, while significant effects of helium appear only at very high concentrations. He implantation levels up to 0.5 at.% He were required to cause a transition from transgranular to completely intergranular brittle fracture mode in 8–9% Cr martensitic steels (EM10 and T91), implanted at 250 °C as well as 550 °C, and tested at room temperature and at the respective implantation temperature [3]. Therefore it has to be clarified, whether or not the beneficial effect of post-implantation annealing is retained at even higher He concentrations. It also must be assessed whether the recovery effect is retained during further implantation-annealing cycles. Some positive indications in this respect are available from reactor irradiations [7].

(3) Current models to describe irradiation hardening are based on pinning of dislocations by clusters of displacement defects, which may agglomerate during cascade evolution or by subsequent

migration, cf. [20,21]. In the present case the increase in strength after implantation may be ascribed to the high density of 'black-dots', observed by TEM in similar martensitic steels [18]. It has been shown previously that this irradiation induced structure is not stable under straining in tensile tests, experiencing for example strain localisation by sweeping of 'black-dot'-free channels [17,22]. Stress concentration due to channel formation is a tentative explanation of the absence of strain hardening and the reduced ductility during testing. Annealing removes the 'black-dots', apparently partially by the formation of new dislocations, as indicated by their increased density [14]. In the tensile test, this annealed structure shows a higher strength than the original material due to the higher dislocation density. On the other hand, the new dislocations also contribute to strain-hardening and increased ductility. Further elaboration of this model requires more quantitative investigations of cluster evolution by TEM and other methods, e.g. small-angle neutron scattering (SANS) or positron annihilation spectroscopy (PAS).

7. Conclusions

- Ductility of helium-implanted EUROFER97 is recovered by post-implantation annealing at 550 °C and 750°, with overall tensile properties being superior after annealing, even compared to material in original condition.
- More investigations are needed for a detailed understanding of the underlying processes.
- Heat treatment of structural parts in nuclear devices after irradiation – although technically demanding – would be rewarding, considering the economical and environmental benefits. The exact heat treatment conditions to obtain the optimum properties still need to be determined.

References

[1] R.L. Klueh, D.J. Alexander, J. Nucl. Mater. 218 (1995) 151.
[2] R. Lindau, A. Möslang, D. Preininger, M. Rieth, H.D. Röhrig, J. Nucl. Mater. 271–272 (1999) 450.
[3] P. Jung, J. Henry, J. Chen, J.-C. Brachet, J. Nucl. Mater. 318 (2003) 241.
[4] P. Jung, J. Henry, J. Chen, J. Nucl. Mater. 343 (2005) 275.
[5] R.L. Klueh, D.R.Harris, High-chromium ferritic and martensitic steels for nuclear applications, ASTM, Stock number: MONO3, 2001.
[6] C. Wassilev, K. Ehrlich, J. Nucl. Mater. 191–194 (1992) 850.
[7] Y.I. Zvezdin, O.M. Vishkarev, G.A. Tulyakov, Y.G. Magerya, V.A. Smirnov, I.A. Shenkova, I.V. Altovski, A.A. Grigoryan, V.K. Shamardin, U.M. Pecherin, J. Nucl. Mater. 191–194 (1992) 855.
[8] V.S. Khabarov, A.M. Dvoriashin, S.I. Porollo, J. Nucl. Mater. 233–237 (1996) 236.
[9] B.N. Singh, D.J. Edwards, P. Toft, J. Nucl. Mater. 299 (2001) 205.
[10] S.A. Fabritsiev, A.S. Pokrovsky, J. Nucl. Mater. 307 (2002) 431.
[11] D.J. Edwards, B.N. Singh, Q. Xu, P. Toft, J. Nucl. Mater. 307 (2002) 439.
[12] S.A. Fabritsiev, A.S. Pokrovsky, S.E. Ostrovsky, J. Nucl. Mater. 324 (2004) 23.
[13] J. Henry, X. Averty, Y. Dai, P. Lamagnère, J.P. Pizzanelli, J.J. Espinas, P. Wident, J. Nucl. Mater. 318 (2003) 215.
[14] J. Chen, P. Jung, M. Rödig, H. Ullmaier, G.S. Bauer, J. Nucl. Mater. 343 (2005) 227.
[15] J.P. Biersack, L.G. Haggmark, Nucl. Instrum. Meth. 174 (1980) 93;
J.F. Ziegler, Manual of TRIM Version 95.4, March 1995, unpublished.
[16] P. Jung, Phys. Rev. B 23 (1981) 664.
[17] H. Ullmaier, J. Chen, J. Nucl. Mater. 318 (2003) 228.
[18] J. Henry, M.-H. Mathon, P. Jung, J. Nucl. Mater. 318 (2003) 249.
[19] A. Kohyama, K. Hamada, H. Matsui, J. Nucl. Mater. 179–181 (1991) 417.
[20] G.E. Lucas, J. Nucl. Mater. 206 (1993) 287.
[21] B.N. Singh, A.J.E. Foreman, H. Trinkaus, J. Nucl. Mater. 249 (1997) 103.
[22] Y. Dai, X. Jia, J.C. Chen, W.F. Sommer, M. Victoria, G.S. Bauer, J. Nucl. Mater. 296 (2001) 174.